AAS 23-434

ACHIEVING SOLAR PRESSURE EQUILIBRIUM ATTITUDE USING SOLAR ARRAY FEATHERING

Benjamin Asher* **and Matthew M. Wittal**†

Many competing requirements such as communication margin, thermal mitigation, and power generation may drive a specific flight attitude. However, a solar pressure equilibrium attitude (SPEA) is typically desired for a spacecraft in heliocentric space in order to minimize attitude maintenance. In this work, the benefits of solar array feathering in order to maintain specific and precise pointing requirements are quantified. A case study in which an asymmetrical spacecraft exploits a normally unstable flight attitude in concert with solar array feathering is explored in order to optimize power utilization while still minimizing attitude maintenance.

INTRODUCTION

As NASA expands to the Moon and Mars through the Artemis campaign, demand for space infrastructure and logistics continues to grow [1–4]. A solution to this demand is the concept of a tug-cargo spacecraft configuration, in which the tug portion may transport modules, fuel, cargo, and satellites to their respective destinations. Like any spacecraft mission design, the tug-cargo configuration comes with its own challenges [5]. A tug is a conceptual, self-sufficient spacecraft with excess power and propulsion which it is capable of providing to a powered payload.

One of the challenges of the tug is that the center axis of the solar arrays does not pass through the combined center of gravity (CG) of the combined tug-cargo configuration. This asymmetry results in a torque acting on the spacecraft due to solar radiation pressure (SRP) which is undesirable for attitude maintenance. The only attitude where there is no torque from SRP is when the spacecraft is in a solar pressure equilibrium attitude (SPEA) as is being done in the mission planning of Gateway.[6,7]

Most missions can vary the spacecraft design to mitigate the torque from SRP, but the tug only has its solar arrays available. There exists other work in the area of solar sail missions[8–10] that utilize SRP for attitude control as well as propulsion. Unfortunately, the unique geometry of a solar sail spacecraft does not apply directly to the tug scenario, however we can learn from their experience in order to better inform the mission design in this work.

The goal of this paper is to derive an analytical relationship between the solar array feathering angle, θ, and the angle of attack of the spacecraft relative to the tug-Sun direction, α, such that given any angle α the solar array feathering angle θ can be determined to result in a net zero torque for any tug-cargo spacecraft configuration. This can turn any attitude into SPEA at the expense of power generation which opens our design space to account for other mission design constraints such as thermal control, communication, and power management.

PRELIMINARIES

The approach is to start with some simplifying assumptions and add fidelity. This approach has been selected in order to derive the solution analytically instead of numerically. Two scenarios are considered.

*Mission Design Engineer, Aegis Aerospace, NASA Kennedy Space Center FL, 32899
†Technologist, Deep Space Logistics, NASA Kennedy Space Center, FL 32899, and Ph.D. Candidate, Embry-Riddle Aeronautical University, 1 Aerospace Blvd., Daytona Beach, FL 32114

- **Scenario 1:** Assume a perfectly reflective material that will help us to simplify our initial equations. Here all of the momentum of incoming solar particles is perfectly reflected resulting in a net force perpendicular to the surface.
- **Scenario 2:** More realistic coefficients of reflectivity are used and the resulting force from the SRP is no longer perpendicular to the surface. The flat plate model within FreeFlyer* will be used and the results will be compared to the simplified model. Here the resulting translational force on the body will be ignored but can be a topic of future study.

In both scenarios, the material properties of the tug body and cargo are considered to be uniform. The material properties of the solar arrays can vary from the body but are considered symmetrical across the two solar arrays.

The Solar Pressure Equilibrium Attitude (SPEA) is defined as when the sum of the torques from SRP is zero. This gives the problem setup of

$$0 = \vec{C}_{P_{side}} \times \vec{F}_{side} + \vec{C}_{P_{top}} \times \vec{F}_{top} + \vec{C}_{P_{SA}} \times \vec{F}_{SA} \tag{1}$$

Where $\vec{C}_{P_i}$ is the center of pressure location with respect to the CG and $\vec{F}_i$ is the SRP force vector. The equation for $\vec{F}_i$ assuming a flat plate is given by[11]

$$\vec{F}_{SRP} = PA_{plate} \left\{ 2 \left(\frac{C_{r_{diffuse}}}{3} + C_{r_{specular}} \cos\phi \right) \hat{N} + (1 - C_{r_{specular}}) \hat{U}_{Sun} \right\} \cos\phi \tag{2}$$

With the variable definitions shown in Table 1.

Table 1: Flat-Plate Variable Definition

P	Solar radiation pressure
A_{plate}	Area of flat plate
$C_{r_{diffuse}}$	Coefficient of diffuse reflectivity
$C_{r_{specular}}$	Coefficient of specular reflectivity
ϕ	Angle between the the Sun vector and the surface normal
$\hat{N}$	Surface normal unit vector
$\hat{U}_{Sun}$	Unit vector from the CG to the Sun

The curved surface of the cylinder can be discritized into a sum of small plates aligned parallel to one another using an approach similar to that of the fundamental theorem of calculus. The aim is to integrate each minute flat plate with an area of $h_B r_B \sin(d\psi)$ where $d\psi$ is a small angle about the center axis (z-axis) of the cylinder. Using the small-angle approximation, $\sin(d\psi) = d\psi$. Since only half the cylinder is visible the integral is evaluated from $[-\pi/2, \pi/2]$.

From Eq. 2, cosϕ can be given as a function of ψ and the pitch angle (α). for the curved cylinder wall, $\hat{N} = [\sin\psi, -\cos\psi, 0]$ and $\hat{U}_{Sun} = [0, -\sin\alpha, \cos\alpha]$. This results in, $\cos\phi = \cos\psi\sin\alpha$. For Scenario 1, we are assuming $C_{r_{diffuse}} = 0$ and $C_{r_{specular}} = 1$. All of these assumptions plugged into Eq. 2 for the curved surface of the cylinder to be

$$\vec{F}_{SRP_{side}} = \int_{\frac{-\pi}{2}}^{\frac{\pi}{2}} P h_B r_B \left\{ 2\cos\psi\sin\alpha \left[\sin\psi, -\cos\psi, 0\right] \right\} \cos\psi\sin\alpha \, d\psi$$

*FreeFlyer is a commercial off-the-shelf software application for space mission design, analysis, and operations.

Note that $\hat{N}$ results in a torque about the x and y axes. Due to the symmetry of the cylinder, the sum of the torques about the y axis is cancelled so there is only a resultant torque about the x axis given by the y component of $\hat{N}$. Knowing this, the equation is further simplified to

$$F_{SRP_{side}} = -2Ph_B r_B \sin^2\alpha \int_{\frac{-\pi}{2}}^{\frac{\pi}{2}} \cos^3\psi \, d\psi$$

$$F_{SRP_{side}} = -\frac{8}{3} Ph_B r_B \sin^2\alpha \tag{3}$$

The resulting torque from the end of the cylinder is zero since the force vector passes through the CG. This will not be true when $C_{r_{specular}} < 1$ in Scenario 2.

The solar panels are flat plates so the equation is more straightforward. The difference is that $\cos\phi = \cos\theta$ where θ is the feathering angle of the solar arrays measured with respect to the Sun with $\theta = 0$ being the pointing for optimal power and $\theta = \pm 90$ is edge on to the Sun. The assumption is that the two solar arrays rotate the same which cancels the torque about the y and z axes resulting in a pure torque about the x axis. The resulting equation for a single solar array is

$$F_{SRP_{SA}} = 2Pl_{SA} w_{SA} \cos^2\theta \sin(\theta - \alpha) \tag{4}$$

Again, the torques are about the x axis and we only use the y component of the force which means our moment arm is the z component of the center of pressure for the given surfaces. The z component of the center of pressure is given by z_B and z_{SA} for the body and solar array respectively. Eq. 1 then becomes Eq. 5 when solving for θ.

$$0 = -\frac{8}{3} Ph_B r_B z_B \sin^2\alpha + 2 * \left[2Pl_{SA} w_{SA} z_{SA} \cos^2\theta \sin(\theta - \alpha)\right]$$

$$\cos^2\theta \sin(\theta - \alpha) = \frac{2h_B r_B z_B \sin^2\alpha}{3l_{SA} w_{SA} z_{SA}} \tag{5}$$

Eq. 5 is not separable. A solution should exist for most tug geometries as long as the right hand term is less than 1 but preferably small. This can be interpreted as the ”controllability” since the desire is to have the torque created by the control surface (the denominator) be greater. Another observation is that since there is both a cosine and sine term, two solutions to the problem should exist. A simple function such as *fzero* in MATLAB or a differential corrector can be used to solve for θ. What initial guess should be used by the solver to yield the best value of θ for power generation?

CASE STUDY

To answer that, a notional spacecraft will be designed in order to access the problem in more detail. The physical parameters to be used are shown in Table 2. The spacecraft is assumed to be in a circular, heliocentric orbit one astronomical unit (AU) from the Sun for SRP calculations.

The notional spacecraft configuration is shown in Fig. 1. The figure includes the cargo in light grey, the tug in dark blue, and the solar array in blue. The combined tug-cargo configuration is considered to be a cylinder with a uniform radius of r_B and a combined height of l_B. The solar arrays each have a length and width of l_{SA} and w_{SA} respectively and the center axis is located a distance of z_{SA} from the CG.

Using the spacecraft design parameters from Table 2, a plot of θ vs. α can be generated to help solve for θ. Some sample values of α are shown in Fig. 2. Note that the equation was manipulated in order to use MATLAB's *fzero* function.

Fig. 2 shows the two different solutions to θ for a given α. As was stated earlier, the value of θ closest to 0 is desired. Fig. 3a shows a plot solving for θ using Eq. 5 as well as selecting the ”best” value of θ.

Note that the ”original” solution shown in Fig. 3a trends very linearly with an oscillating term. The slope of the best fit linear trend line is very similar to Eq. 6.

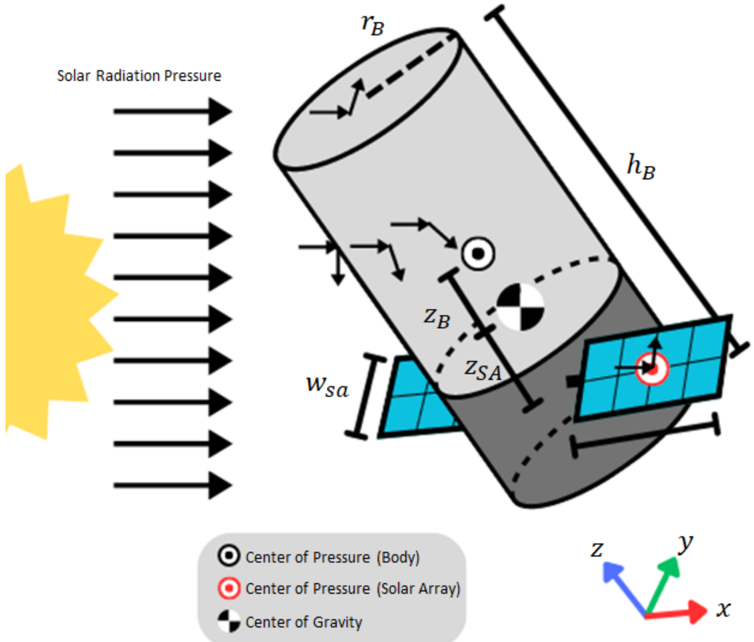

Figure 1: Definition of terms for spacecraft in SPEA configuration.

Table 2: Tug-Cargo Properties

Spacecraft Geometry	
Combined height of the cargo and tug [m]	$h_B = 8$
Radius of the cargo and tug [m]	$r_B = 1.8$
z component of the center of pressure of the body [m]	$z_B = 0.8$
Length of each solar array [m]	$l_{SA} = 5.4$
Length of each solar array [m]	$w_{SA} = 2.7$
z component of the center of pressure of the solar arrays [m]	$z_{SA} = 1$
Scenario 1 Material Properties	
Body (Diffuse)	$C_{r_{diffuse}} = 0$
Body (Specular)	$C_{r_{specular}} = 1$
Solar Array (Diffuse)	$C_{r_{diffuse}} = 0$
Solar Array (Specular)	$C_{r_{specular}} = 1$
Scenario 2 Material Properties	
Body (Diffuse)	$C_{r_{diffuse}} = 0.1$
Body (Specular)	$C_{r_{specular}} = 0.8$
Solar Array (Diffuse)	$C_{r_{diffuse}} = 0.1$
Solar Array (Specular)	$C_{r_{specular}} = 0.5$

$$1 - \frac{2h_B r_B z_B}{3l_{SA} w_{SA} z_{SA}} \tag{6}$$

More studying is needed to confirm the relationship but it turns out to be great as an initial guess in the solver. The goal would be to determine an explicit equation to solve for θ that could be used onboard a spacecraft for control instead of requiring a computationally expensive solver or relying on commands from the ground.

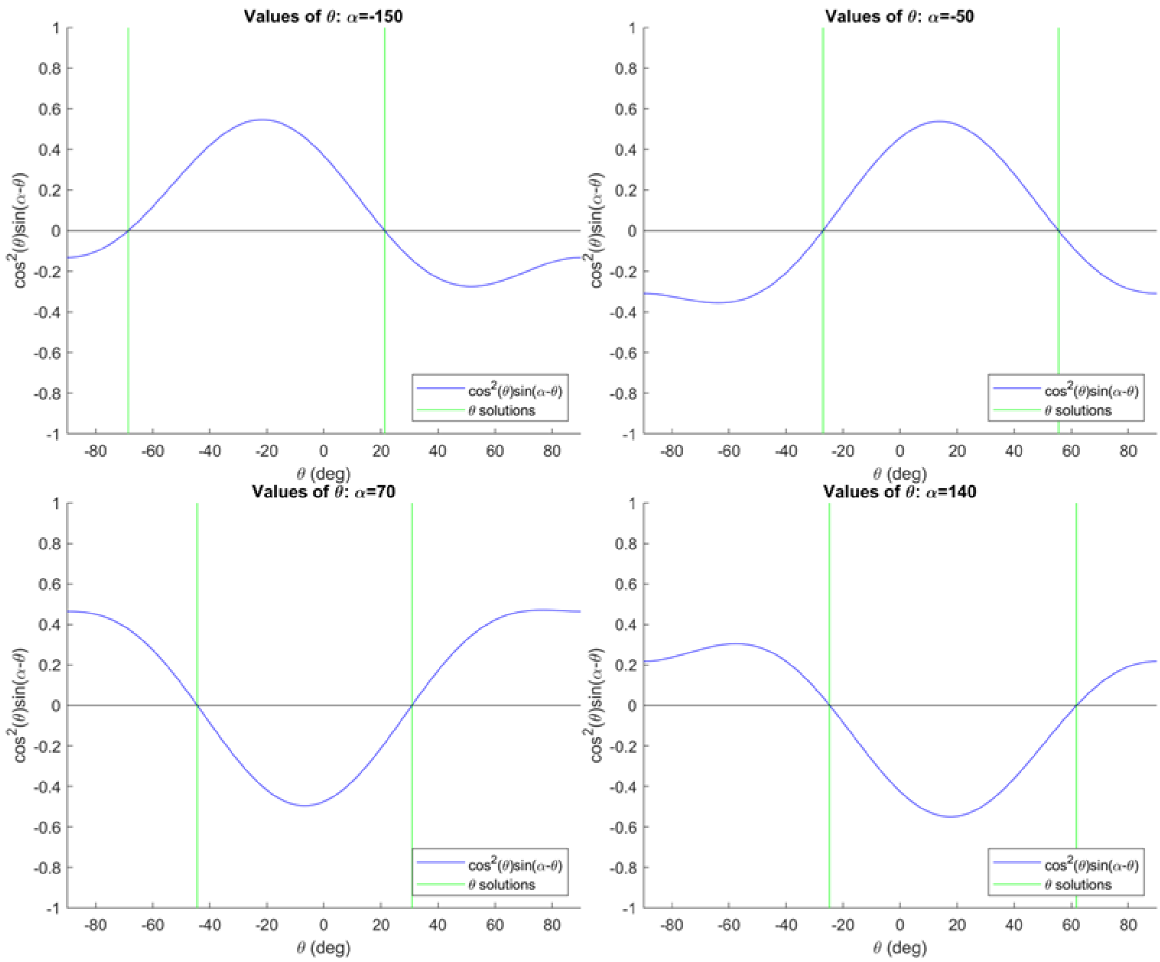

Figure 2: How the value of θ changes with respect to Eq. 5.

RESULTS

For this notional spacecraft the maximum value of θ is 36.14 deg when α is at 90 deg. This feathering angle results in a cosine loss of just under 20%. This is a scenario where the tug-cargo spacecraft would desire to fly broadside to the Sun which would help warm the cargo. Depending on the size of the cargo this could reduce the power demand from heaters on the cargo by more than 20% compared to a nose-to-Sun attitude, resulting in a an overall power savings while maintaining SPEA and minimizing the demand on the reaction control system.

A more realistic spacecraft has yet to been considered to determine if the statements made above are true as fidelity is added to the model. Fig. 3b shows a comparison of the idealized model versus one using more realistic material properties as shown in Table 2.

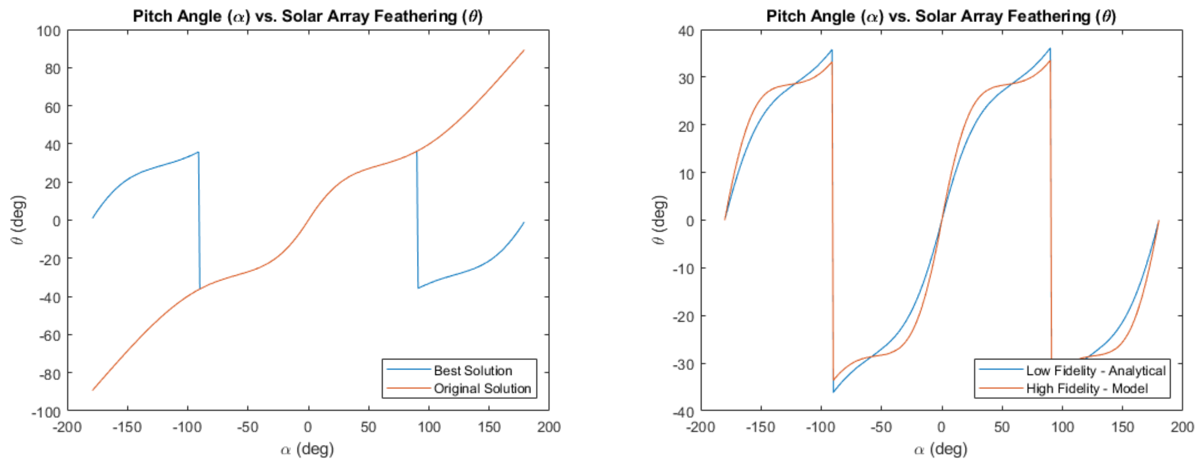

(a) Scenario 1 (b) Scenario 2

Figure 3: SPEA attitude as a function of solar array feathering.

The derivation of the higher fidelity model is a topic for future work, but it still trends similarly to the idealized model. Perhaps different surface material properties can be designed if any Sun relative attitude constraints are known in advance in order to minimize the amount of feathering needed. For example in the range of -50 to 50 degrees of α, a more reflective surface would be desired while values of α ranging from 50 to 90 degrees a material with more absorbance would be desired.

CONCLUSION

A design space for tug-cargo spacecraft was explored to enable solar pressure equilibrium attitudes using solar array feathering. Solutions were shown that did not require excessive feathering of the solar arrays opening a design space previously not considered. This work serves as a proof of feasibility and can serve as a foundation for future studies using solar arrays for attitude control.

At least for the simple cylindrical geometry shown here, the idealized model can be used for preliminary studies. Future studies would include the derivation of the equations for a higher fidelity model which includes more complex geometries and different CG locations. The concept of using the solar arrays actively for both attitude control and translational motion similar to solar sails may even be considered with future missions concepts.

REFERENCES

[1] H. Chen and K. Ho, "Integrated Space Logistics Mission Planning and Spacecraft Design with Mixed-Integer Nonlinear Programming," *Journal of Spacecraft and Rockets*, Vol. 55, No. 2, 2018, pp. 365–381.

[2] H. Chen, K. Ho, B. Gardner, and P. Grogan, *Built-in Flexibility for Space Logistics Mission Planning and Spacecraft Design*.

[3] M. Wittal, J. Smith, and A. Cassell, "Mission Design Considerations for Robotic Lunar and Gateway Payload Return," *AIAA/AAS Astrodynamics Specialist Conference*, No. AAS 21-724.

[4] M. Wittal, S. Miaule, and B. Asher, *Earth-Moon Cycler Mission Design for Lunar Logistics*. No. AC-22-C1.6.6.

[5] V. Hutchinson and K. Bocam, "Space Tug: An Alternative Solution to ISS Cargo Delivery," *AIAA SPACE 2009 Conference & Exposition*.

[6] C. P. Newman, D. C. Davis, R. J. Whitley, J. R. Guinn, and M. S. Ryne, "Stationkeeping, Orbit Determination, and Attitude Control for Spacecraft in Near Rectilinear Halo Orbits," *AAS 18-388*, 2018.

[7] NASA/SP-8027, *NASA Space Vehicle Design Criteria (Guidance and Control): Spacecraft Radiation Torques*. (Monograph), OCT-1969.

[8] D. C. Ullery, S. Soleymani, A. Heaton, J. Orphee, L. Johnson, R. Sood, and P. Kung, "Strong Solar Radiation Forces from Anomalously Reflecting Metasurfaces for Solar Sail Attitude Control," 2018.

[9] B. L. Diedrich, "Attitude Control and Dynamics of Solar Sails," 2001.

[10] B. Stuck, "Solar Pressure Three-Axis Attitude Control," *Journal of Guidance Control and Dynamics*, Vol. 3, 03 1980, pp. 132–139.

[11] D. A. Vallado, *Fundamentals of Astrodynamics and Applications, 3rd edn.* Microcosm Press, Hawthorne and Springer, 2007.